The Sunyaev-Zeldovich Effect

Y. Rephaeli([1])([2]), S. Sadeh([1]) and M. Shimon([1])([2])

([1]) *School of Physics & Astronomy, Tel Aviv University, Tel Aviv, Israel*

([2]) *Center for Astrophysics and Space Sciences, UCSD, La Jolla, CA, USA*

1. – Introduction

During passage through a cluster of galaxies some of the photons of the cosmic microwave background (CMB) radiation are scattered by electrons in the hot intracluster (IC) gas. The scattering slightly modifies the incident Planck spectrum, imprinting on it a unique spectral signature that was first described by Sunyaev & Zeldovich (1972). [The impact of hypothetical hot intergalactic gas on the CMB spectrum was calculated earlier by Weymann (1966) and Zeldovich & Sunyaev (1969).] This Sunyaev-Zeldovich (S-Z) effect is a valuable tool for probing the cluster environment and the global properties of the universe. The basic significance of the effect was pointed out in the early work of Sunyaev & Zeldovich, and in many papers written during the first decade following their original paper. General reviews of the effect and its measurements include those by Rephaeli (1995a), Birkinshaw (1999), and Carlstrom et al. (2002).

The major challenge of measuring the effect in nearby clusters was taken up soon after the effect was identified, but some decade and a half passed before convincing detections were made. Observational results from single-dish radio measurements were reviewed by Birkinshaw (1999). Growing realization of the cosmological significance of the effect has led to major improvements in observational techniques, and to extensive theoretical investigations of its many aspects. The use of interferometric arrays and the substantial progress in the development of sensitive radio receivers led to first interferometric images of the effect (Jones et al. 1993, Carlstrom et al. 1996). Some 60 clusters have already been imaged with the OVRO and BIMA arrays (Carlstrom et al. 2002).

With the many S-Z projects that will become operational in the very near future, measurements of the S-Z effect are about to expand tremendously. The effect is expected to be detected in thousands of clusters when planned cluster surveys are conducted. For many clusters we expect to have detailed spatial mapping of the effect. Together with the much expanded spectral coverage, a large S-Z database will greatly advance our ability to fully exploit the potential of using the effect as a *precise* cosmological probe. The main observational challenges in precision S-Z work are discussed in the review of Birkinshaw in this volume. As noted, general reviews are available of the S-Z effect and the main observational results. Our brief review here is meant to be somewhat more pedagogical.

2. – The Effect

The spectral change resulting from Compton scattering of the CMB by IC gas was calculated by Sunyaev & Zeldovich (1972) in the non-relativistic limit based on a solution to the Kompaneets equation (which essentially is a diffusion approximation to the exact kinetic equation). As was clearly demonstrated by Rephaeli (1995b), the approximate (though elegantly simple) expressions for the intensity change, ΔI, obtained by Sunyaev & Zeldovich (eqs. 6-9) are not sufficiently accurate at high frequencies and temperatures. IC gas temperatures span the range $3-15$ keV; high electron velocities result in relatively large photon energy change in the scattering, requiring a more exact relativistic calculation.

2˙1. Total Intensity Change. – Using the exact probability distribution, and a relativistically correct form of the electron Maxwellian velocity distribution, Rephaeli (1995b) calculated the resulting intensity change in the limit of small optical depth to Thomson scattering, τ, keeping terms linear in τ. In this semi-analytic treatment for the calculation of ΔI_t – the change of intensity due to scattering by electrons with a thermal velocity distribution – the starting point is the probability of scattering of an incoming photon (direction $\mu_0 = \cos\theta_0$) to the direction $\mu_0' = \cos\theta_0'$ is (Chandrasekhar 1950)

$$f\left(\mu_0,\mu_0'\right) = \frac{3}{8}\left[1+\mu_0^2\mu_0'^2+\frac{1}{2}\left(1-\mu_0^2\right)\left(1-\mu_0'^2\right)\right] \tag{1}$$

where the subscript 0 refers to the electron rest frame. The resulting frequency shift is

$$s = \ln\left(\nu'/\nu\right) = \ln\left(\frac{1+\beta\mu_0'}{1+\beta\mu_0}\right) \tag{2}$$

where ν, ν' are the photon frequency before and after the scattering, and $\beta = v/c$ is the dimensionless electron velocity in the CMB frame. It is somewhat more convenient to use the variables μ, s and β instead of μ, μ' and β. The probability that a scattering results in a frequency shift s is (Wright 1979)

$$\mathcal{P}\left(s,\beta\right) = \frac{1}{2\gamma^4\beta}\int\frac{e^s f\left(\mu_0,\mu_0'\right)}{\left(1+\beta\mu_0\right)^2}d\mu_0. \tag{3}$$

Averaging over a Maxwellian distribution for the electrons yields

$$\mathcal{P}_1\left(s\right) = \frac{\int\beta^2\gamma^5 e^{-\frac{(\gamma-1)}{\Theta}}\mathcal{P}\left(s,\beta\right)d\beta}{\int\beta^2\gamma^5 e^{-\frac{(\gamma-1)}{\Theta}}d\beta}, \tag{4}$$

where $\Theta = kT_e/m_ec^2$. The total change in the photon occupation number along a line of sight (los) to the cluster can now be written as

$$\Delta n_t(x) = \tau\int_{-\infty}^{\infty}\left[n\left(xe^s\right)-n\left(x\right)\right]\mathcal{P}_1\left(s\right)ds \tag{5}$$

where x is the dimensionless frequency, $x = h\nu/kT$, T is the CMB temperature, the optical depth is $\tau \equiv \sigma_T\int n_e dl$, and σ_T is the Thomson cross section. The change of intensity is simply calculated using $\Delta I_t(x) = i_o x^3\Delta n_t(x)$, where $i_o = 2(kT)^3/(hc)^2$.

In the nonrelativistic limit the Kompaneets eq. can be readily solved leading to a simple analytic expression (Sunyaev & Zeldovich 1972) for ΔI_t,

$$\Delta I_t = i_o y g(x) \ , \tag{6}$$

where the dependence on the cluster gas density (n) and temperature is in the Comptonization parameter (essentially, an integral over the electron pressure),

$$y = \int (kT_e/mc^2) n \sigma_T dl \ . \tag{7}$$

The spectral function

$$g(x) = \frac{x^4 e^x}{(e^x-1)^2} \left[\frac{x(e^x+1)}{e^x-1} - 4 \right] , \tag{8}$$

is negative for $x < 3.83$ and positive at larger values of this crossover frequency, ~ 217 GHz. The magnitude of the relative temperature change due to the thermal effect is $\Delta T_t/T = -2y$ in the R-J region, with $y \sim 10^{-4}$ along a line of sight (los) through the center of a rich cluster.

The motion of the cluster in the CMB frame induces a *kinematic* (Doppler) S-Z component, which can be easily calculated in the nonrelativistic limit (Sunyaev & Zeldovich 1980)

$$\Delta I_k = -i_o \tau \beta_c h(x) \ , \quad h(x) = \frac{x^4 e^x}{(e^x-1)^2} \ , \tag{9}$$

where $\beta_c = v_r/c$, with v_r the line of sight component of the cluster peculiar velocity. The corresponding temperature change for this kinematic component is $\Delta T_k/T = -\tau\beta_c$.

The results of the relativistic and nonrelativistic calculations of $\Delta I_t(x)$ are shown in fig. 1 for $kT_e = 5, 10, 15$ keV. As is evident, the more accurate relativistic calculation yields values that are appreciably different from those based on the nonrelativistic formula. The deviations increase with T_e and are particularly large near the crossover frequency, where the purely thermal effect vanishes. This frequency shifts to higher values with increasing T_e. Also, while the dependence ΔI_t on τ is still linear to a high degree of accuracy, its dependence on T_e is sufficiently non-linear (for typical values of T_e) that the intensity change should no longer be determined through the use of the Comptonization parameter y.

While most S-Z observations have traditionally been at (relatively) low frequencies ($\sim$ 30 GHz, or $x \sim 0.5$) where the approximate nonrelativistic description is roughly adequate, some 16 clusters were observed also at much higher frequencies (with, *e.g.*, the SuZIE and MITO telescopes, up to $x \sim 6.2$). In fact, most future S-Z projects will observe the effect at several high frequencies. Use of the relativistically exact expressions for ΔI_t and ΔI_k is clearly necessary at $\nu >> 30$ GHz, especially when the effect is used to determine precise values of cluster and cosmological parameters. Moreover, since the ability to measure peculiar velocities of clusters depends very much on observations very close to the crossover frequency, its dependence on T_e, which is approximately given (Shimon & Rephaeli 2004) in

$$x_0 \simeq 3.8300(1 + 1.1206\theta + 2.0783\theta^2 - 80.7481\theta^3), \tag{10}$$

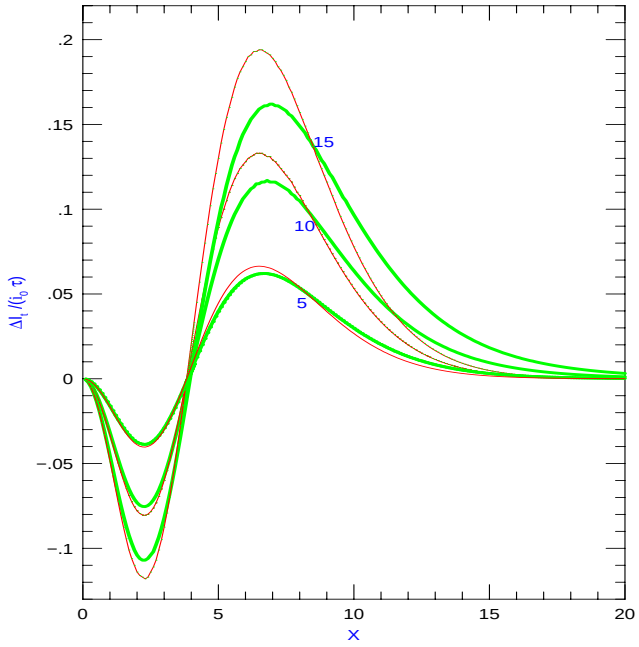

Fig. 1. – The spectral distribution of $\Delta I_t/(i_o\tau)$. The pairs of thick (green) and thin (red) lines, labeled with $kT_e = 5$, 10, and 15 keV, show the relativistic and nonrelativistic distributions, respectively.

should be taken into account. Note also that because high precision S-Z work entails use of X-ray derived gas parameters, similarly accurate expressions for the X-ray bremsstrahlung emissivity have to be employed (Rephaeli & Yankovitch 1997). In the latter paper first order relativistic corrections to the electron velocity distribution and electron-electron bremsstrahlung were taken into account in correcting values of the Hubble constant, H_0, that were previously derived using the nonrelativistic expression for the emissivity (see also Hughes & Birkinshaw 1998, and Nozawa et al. 1998b).

The calculation of Rephaeli (1995b) motivated various generalizations and extensions of the relativistic treatment. Challinor & Lasenby (1998) obtained an analytic approximation to the solution of the relativistically generalized Kompaneets equation, whose accuracy was then extended to fifth order in Θ (Nozawa et al. 1998a). Sazonov & Sunyaev (1998) and Nozawa et al. (1998b) have extended the relativistic treatment also to the kinematic component obtaining (for the first time) the leading cross terms in the expression for the combined (thermal and kinematic) intensity change, $\Delta I_t + \Delta I_k$, which depend on both T_e and v_r. Since in some rich clusters $\tau \sim 0.02 - 0.03$, sufficiently accurate analytic expansions of the expression for ΔI in powers of $\Theta = kT_e/mc^2$ necessitate the (consistent) inclusion also of multiple scatterings of order τ^2 (Molnar & Birkinshaw 1999, Itoh et al. 2000, Shimon & Rephaeli 2004). Details on the calculation of the full effect are given in these papers.

The exact relativistic calculation of ΔI does not lead to a simple analytic expression. In order to obtain an approximate analytic expression (that can greatly simplify the analysis of S-Z measurements), one needs to expand the formal expression for ΔI in powers of (the small quantities) τ, Θ, and β_c. For the resulting expression to be accurate to within to $\sim 2\%$ for $kT_e < 50$ keV, Shimon & Rephaeli (2004) included terms up to $\tau\Theta^{12}$, $\tau^2\Theta^5$, and $\beta_c^2\Theta^4$. [Itoh & Nozawa (2004) have derived a slightly more accurate fit to the results of the exact numerical calculation; however, results of this fit are given in terms of an array of tabulated coefficients.] Since cluster velocities are expected to be generally well below 1000 km/s, terms quadratic in β_c can be ignored. Doing so we can write the total intensity change as the sum

$$\Delta I/i_o = \tau\sum_{j=1}^{8} f_j(x)\Theta^j + \tau^2\sum_{j=1}^{4} f_{j+8}(x)\Theta^{j+1} - \tau\beta_r\left[h_0(x) + \sum_{j=1}^{4} f_{j+12}(x)\Theta^j\right], \tag{11}$$

where $f_j(x) = x^3F_j(x)$, with $F_j(x)$ defined in Shimon & Rephaeli (2004).

2˙2. Polarization Components. – Due to the particular angular dependence of the cross section, incident unpolarized radiation is linearly polarized if it has a finite quadrupole moment. The polarization - which is described in a plane orthogonal to the los - is completely specified by the Q and U Stokes parameters. Axial symmetry of the scattering (as is evident from the dependence of the frequency change, Equation 2, on θ, θ' but not on ϕ or ϕ') allows the freedom to select a frame such that $U = 0$. [Note that this is no longer the case in the presence of a magnetic field (*e.g.* Ohno et al. 2003) or when the cluster substructure is spatially resolved (Shimon et al. 2005).] Using the above notation Q can be written as

$$Q(\mu) = \frac{3}{8}\tau(1-\mu_0^2)\int_{-1}^{1} P_2(\mu_0')I(\mu_0')d\mu_0', \tag{12}$$

where $P_2(\mu_0')$ is the second Legendre polynomial. From the orthogonality of the Legendre polynomials it is clear that Q depends only on the quadrupole moment of the incident radiation as observed in the electron rest frame.

CMB polarization resulting from Compton scattering in clusters was first considered by Sunyaev & Zeldovich (1980). Using Equation (12) they obtained, to first order in τ,

$$Q_1 = \frac{\tau}{20}\beta_t^2\frac{xe^x(e^x+1)}{(e^x-1)}, \tag{13}$$

and to second order

$$Q_2 = \frac{\tau^2}{40}\beta_t. \tag{14}$$

Both components, which are given here in (temperature) K, depend only on the tangential velocity of the cluster, $c\beta_t$, and thus their measurement provides complementary velocity information to (the leading term in) the kinematic S-Z effect, which depends on the los velocity.

The proportionality of Q_1 to β_t^2 follows from its dependence on the second derivative of the Planck distribution, while Q_2 is proportional to its first derivative. This feature

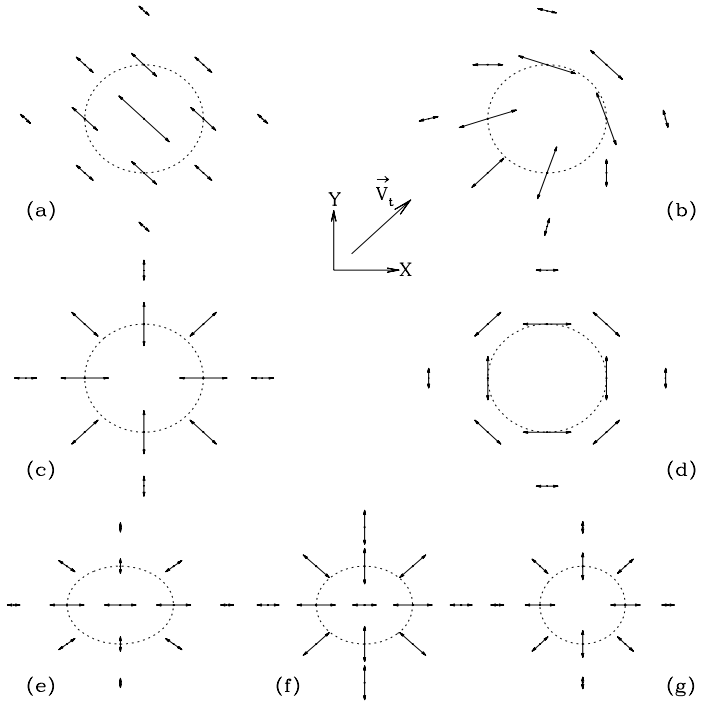

Fig. 2. – Patterns of the polarization components described in the text. In cases (a)–(d) β-profile with $\beta = 3/2$ is assumed, and the cluster peculiar velocity is as indicated by the arrow $\vec{V}_t$. (a) The $\propto \beta_t^2\tau$ component. (b) The $\propto \beta_t\tau^2$ component. (c) The thermal component $\propto (kT_e/m_ec^2)\tau^2$ at frequencies $x < 3.83$, and (d) at $x > 3.83$. Elliptical cluster with the ratio of the principal axes $b/a = 0.8$ and the symmetry (longer) axis in the X direction (e), the symmetry axis inclined at 45° to the picture plane (f), and with the symmetry axis along the line of sight (g). Figure adopted from Sazonov & Sunyaev (1999).

renders these two effects distinguishable through multi-frequency observations. Moreover, due to the different dependence on the optical depth, the two effects are expected to be distinguishable by their different spatial signatures in spherical clusters; these are shown in fig. 2a & 2b), along with some of the other polarization components that were calculated and described by Sazonov & Sunyaev (1999) and mentioned briefly below. Corrections to the $\propto \tau\beta^2$ component (Equation 13) due to the random (thermal) component of electron velocity were calculated by Challinor, Ford & Lasenby (2000), and Itoh et al. (2000). These corrections generally amount to $\sim 10\%$ reduction in Q_1.

Another polarization component is due to multiple scatterings; the first scattering induces the requisite quadrupole moment; the radiation is polarized upon second scattering. This component is proportional to $\tau^2\Theta$ (figs. 2c & 2d).

In addition to the above polarization components due to quadrupole moments associated with electron motions (both directed and random), polarization arises also from the intrinsic CMB quadrupole of the primary anisotropy. This achromatic component is $\frac{\tau}{10}\sqrt{\frac{15}{2\pi}C_2}$, where $\sqrt{C_2}$ is the quadrupole moment of the CMB power spectrum,

$\sqrt{C_2} \sim 1.9 \times 10^{-5}$). The magnitude of this component is typically ~ 20 nK; although small, it could possibly be distinguished from the other components by its random distribution over the sky. It was proposed that the dependence of this polarization component on C_2 can be used to reduce cosmic variance (Kamionkowski & Loeb 1997), and that the evolution of C_2 with redshift provides a mean to probe dark energy models (Cooray & Baumann 2003).

In the calculations of the above polarization components it is usually assumed that the cluster is spherically symmetric. If the cluster is ellipsoidal the optical depth is anisotropic and the polarization patterns are as shown in figs. 2e-2g.

Measurement of polarized S-Z signals has been a major challenge so far. Based on the expected high sensitivity and high spatial resolution of upcoming polarization experiments, the detection of the major signals is projected to be feasible. This has motivated more detailed studies of CMB polarization taking into consideration the complex morphology of evolving clusters that can be followed in hydrodynamical simulations. For example, Diego, Mazzotta & Silk (2003) and Lavaux et al. (2004) explored the polarization induced by bulk motions during merging of subclusters. The fact that both the magnitudes and spatial patterns of polarized cluster signals cannot be realistically explored in the context of idealized gas density and temperature distributions was made clear by the work of Shimon et al. (2005). In their paper the leading polarization components ($\propto \tau^2\Theta$, $\propto \tau\beta^2$ and $\propto \tau^2\beta$) were calculated in a rich cluster simulated by the Enzo code. The maximal polarization levels were found to be a few tenths of a μK, with patterns that are considerably more complex than predicted by the idealized calculations whose results are shown in fig. 2.

In addition to polarization in individual clusters the impact of the cluster population on the CMB polarization is of considerable interest. This has been studied by, *e.g.* Hu (2000), and is discussed by Cooray, Baumann & Sigurdson in this volume.

3. – Power Spectrum & Cluster Counts

It has been realized early on that the scattering of the CMB in clusters induces spatial anisotropy (Sunyaev 1977) whose basic properties were already determined in the context of a simple model for the distribution of clusters and the evolution of IC gas (Rephaeli 1981). More than two decades later it is now well established that this is the most important secondary anisotropy on arcminute scales. Since the anisotropy arises from scattering of the CMB in the evolving population of clusters, its power spectrum and cluster number counts can potentially yield important information on the properties of IC gas, the cluster mass function, cosmological evolution of clusters and their gaseous contents, as well as some of the global cosmological and large scale structure parameters. Clearly, therefore, the detailed description of this anisotropy necessitates also the additional modeling of gas properties across the evolving population of clusters.

The traditional approach to the calculation of the S-Z anisotropy is based on the Press-Schechter model for the cluster mass function, $n(M, z)$, the comoving density of clusters of mass M at redshift z. Following collapse and virialization, IC gas is presumed to have reached hydrostatic equilibrium at the virial temperature, with a density distribution that is commonly assumed to have an isothermal β profile. The mass function is normalized by specifying the mass variance on a scale of $8h^{-1}$ Mpc, σ_8, a parameter which can be determined from the primary CMB power spectrum, from large-scale galaxy surveys, or from the observed X-ray temperature function when calibrated by a mass-temperature relation (which is currently limited to clusters at relatively low redshifts). The cluster-

induced anisotropy has been studied at an increasingly greater degree of sophistication and detail (and in a range of cosmological and dark matter models) beginning more than a decade ago (*e.g.*, Makino & Suto 1993, Bartlett & Silk 1994, Colafrancesco et al. 1994). For example, in the latter paper the temperature anisotropy was calculated in a flat CDM model including gas evolution. The approach adopted in that paper was later (Colafrancesco et al. 1997) extended to other cosmological models, and to the calculation of the mass and redshift distributions of the many thousands of clusters that are expected to be detected during the planned Planck survey. The anisotropy and its power spectra can also be generated directly from hydrodynamical simulations (*e.g.*, da Silva et al. 2000). And, of course, the range of cosmological models was extended to include currently favored ΛCDM models (beginning with the works of Komatsu & Kitayama 1999, Molnar & Birkinshaw 2000, and Cooray et al. 2000).

The main features of the power spectra of the anisotropy due to the thermal and kinematic S-Z components, and the cluster number counts, were determined already in the above mentioned papers. Given the nature of the required input parameters characterizing the cosmological and cluster models, it is not surprising that the predicted power spectra and number counts span a wide range. We briefly review some of the recent (since 2001) results from analytical calculations and hydrodynamical simulations in ΛCDM models.

Two approaches have been adopted in the calculation of the S-Z induced anisotropy. In the analytic approach clusters are described by simple models, which characterize their morphologies, temperatures, and their gas content and evolution, usually as functions of the virial mass and redshift. For each cluster the profile of the Comptonization parameter is calculated and transformed into Fourier space. The overall power spectrum can then be quantified by convolving the transformed y-parameter with a cosmological mass function characterizing the universal cluster population, traditionally taken to be of the Press & Schechter (1974) form. The power spectrum can then be calculated numerically using the expression

$$C_\ell = \int_z r^2 \, \frac{dr}{dz} \int_M N(M,z)\, \zeta_\ell(M,z)\, dM\, dz, \tag{15}$$

where r is the comoving radial distance to a cluster of mass M located at redshift z, $N(M,z)$ is the mass function, and $\zeta_\ell(M,z)$ is the angular Fourier transform of the ΔT. In the second approach high resolution dynamical and hydrodynamical simulations (incorporating both dark matter and baryonic components) yield large cosmological fields which enable the identification of individual clusters and their properties relevant to the calculation of y, and the S-Z power spectrum.

Of course, these approaches have their respective advantages and drawbacks. Simple analytic modeling in the first approach can be readily implemented in a computer code, and the impact of various input data can be easily assessed. The main disadvantage of this approach is the explicit need for detailed modeling of each component of the calculation, each with its own uncertainties due to either oversimplified physics, or lack of quality data, or both. An example for this is the mass-temperature relation, used to attribute a temperature to a cluster with virial mass M. A favored scaling is the virial relation

$$T = T_0\,(1+z) \left(\frac{M}{10^{15}\, h^{-1}\, M_\odot} \right)^{2/3} \Omega_0^{1/3} \left[\frac{\Delta(\Omega_0, z)}{\Delta(\Omega_0 = 1, z = 0} \right]^{1/3}, \tag{16}$$

where T_0 is the gas temperature of a $10^{15}\,h^{-1}\,M_\odot$ cluster located at redshift $z = 0$, and $\Delta(\Omega_0, z)$ is the non-linear density contrast at redshift z, and h is the value of H_0 in units of 100 km s^{-1} Mpc^{-1}. In addition to the questionable assumption that clusters are relaxed and in hydrostatic equilibrium, there is appreciable uncertainty both in the value of T_0 and the scaling of the temperature with redshift. The main current limitations of cluster hydrodynamical simulations are the inclusion of a restricted range of physical processes, and insufficient spatial resolution.

As consequence of the redshift independence of the S-Z effect the detection of many distant clusters by upcoming projects is very feasible. Obviously, the number of clusters that can in principle be detected depends on both their universal population, internal properties, and the flux detection limit of the experiment. The number of clusters whose S-Z flux exceeds ΔF_ν is

$$N(>\Delta F_\nu) = \int r^2 \frac{dr}{dz} dz \int_{\Delta F_\nu} B(M,z) N(M,z)\, dM. \tag{17}$$

The lower limit of the mass integral corresponds to the limiting flux from a cluster with mass M located at redshift z, and $B(M, z)$ is either unity or zero, depending on whether the flux measured from the cluster is higher or lower than the flux limit of the experiment. Since the detection of clusters through the S-Z effect cannot reveal any information concerning their redshifts, the observable quantity is the cumulative number clusters at all redshifts. Note that just as for the power spectrum, theoretical predictions of cluster number counts span a wide range that reflects the uncertainties in internal properties of clusters and their mass function.

The power spectrum of the S-Z effect in a ΛCDM model has been calculated by numerous authors (e.g. Komatsu & Kitayama 1999, Molnar & Birkinshaw 2000, Cooray et al. 2000, Komatsu & Seljak 2002, Bond et al. 2002, Zhang et al. 2002, Springel et al. 2001) both analytically and from results of simulations. The resulting power spectra have essentially a universal shape - a steep monotonic ascent to a peak followed by a sharp descent, as shown in the (semi-logarithmic) plot in fig. 4. The curves differ, however, in the multipoles at which the peaks fall, the magnitude of the peak power, and - to a lesser extent - the width of the peaks, as detailed in the rest of this section.

The power spectrum was calculated by Molnar & Birkinshaw (1999) for an $\Omega_0 = 0.2$, $\Omega_\Lambda = 0.8$, $h = 0.5$ model, using a Press & Schechter mass function normalized by $\sigma_8 = 1.35$, a density fluctuation spectrum with index $n = -1.4$, and cluster mass range bounded by $M_{min} = 10^{13}\,h^{-1}\,M_\odot$ and $M_{max} = 10^{16}\,h^{-1}\,M_\odot$. Evolving gas fraction was adopted, with the density decreasing according to $\sim (1+z)^{-1}$ at earlier times. An isothermal gas was assumed, with a temperature of $8.7\,keV$ ascribed to a local cluster of mass $10^{15}\,M_\odot$, and a β density profile with $\beta = 1$. The resulting power spectrum peaks at $\ell \sim 2000$, with a peak magnitude of $\ell(\ell+1)/2\pi \cdot C_\ell \sim 10^{-11}$ K^2. Komatsu & Kitayama (1999) employed $\Omega_\Lambda = 0.5$, $\Omega_0 = 0.3$, and $h = 0.7$, similarly modeled the gas profile and mass function, but adopted $\sigma_8 = 1$, $\beta = 2/3$, $M_{min} = 5 \cdot 10^{13}\,h^{-1}\,M_\odot$, and $M_{max} = 5 \cdot 10^{15}\,h^{-1}\,M_\odot$. Moreover, the gas content was assumed to be non-evolving, and the core radius was determined by assuming that the gas is in a minimum entropy phase, which implies an evolving core size. This model was formulated using a free parameter, ϵ, with the values $-1, 0, 1$. The power spectrum peaks at $l \sim 2000 - 4000$, with maximal power in the range $4 - 7 \cdot 10^{-12}\,K^2$ for the three values of ϵ. Note that the spectral function $g(x)$ was divided out, so that in order to compare these results with others calculated in the Rayleigh-Jeans region, where $g(x) = -2$, the power spectrum magnitude must

be multiplied by a factor of 4. Cooray et al. (2000) calculated the power spectrum for an $\Omega_0 = 0.65$, $\Omega_\Lambda = 0.65$ and $h = 0.65$ model, normalized the Press & Schechter mass function with $\sigma_8 = 0.9$, and determined the gas profile from a solution to the hydrostatic equation with an NFW-distributed dark matter profile. The gas was assumed to be non-evolving fraction of the total mass, and isothermal with a (local) $10^{15}\,h^{-1}\,M_\odot$ cluster assigned to have a temperature of $5.2\,keV$. The resulting peak power is $\sim 10^{-11}\,K^2$ at $\ell \sim 2000 - 3000$.

Studies of the S-Z power spectrum based on hydrodynamical simulations include those of Springel et al. (2001), and Bond et al. (2002), who adopted the favored $\Omega_\Lambda = 0.7$, $\Omega_0 = 0.3$, model with $\sigma_8 = 0.9$ and index $n = 1$. The resulting power spectra are broad and peak at considerably higher multipoles of up to ~ 10000, with peak power that is also somewhat higher than calculated analytically. (Similar results were obtained also by Zhang et al. 2002.)

As an example of how different models may lead to different power predictions we show in fig. 3 a comparison of power spectra calculated with three different mass functions, Press & Schechter (1974), Lee & Shandarin (1999), Sheth & Tormen (1999), hereafter PS, LS and ST, respectively. While the PS and ST mass functions seem to yield approx-

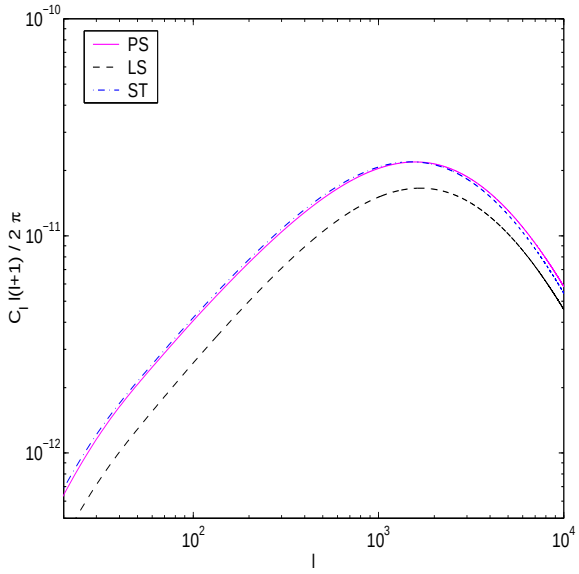

Fig. 3. – Dependence of the S-Z power spectrum on the choice of mass function.

imately the same results, the LS mass function generates lower magnitude power at all multipoles by $\sim 30 - 50\%$.

From these and numerous other published results it is clear that the predicted power spectra span a wide range of values for the width of the peak and its magnitude, reflecting mostly (but not only) different assumed values $\sigma_8 = 0.9$ and gas properties. The impact of a particular choice of parameters on the peak power and its typical scale (ℓ) can be readily predicted. Well known is the steep dependence of the power on σ_8 (fig. 4), due to its location in the exponential part of the mass function; various studies have shown that even a mild change of $\sim 10\%$ may lead to an order of magnitude difference in the

magnitude of the power spectrum. On the other hand, the spectrum is much less sensitive to other cosmological parameters, such as Ω_m, implying that the uncertainty in σ_8 is of major relevance to precise determination of the power spectrum. The impact of different choices of IC gas properties can be easily anticipated; for example, an increase of either the normalization of the mass-temperature relation or the central electron density by a factor f, would lead to an increase of power by a factor f^2, since the power spectrum is proportional to y^2. A steeper y profile - as is obtained in polytropic gas models - shifts power towards higher multipoles since the effective size of the cluster decreases (Sadeh & Rephaeli 2004). This is also the case if the gas is assumed not to evolve with redshift, since this leads to an increase in the population of distant, smaller clusters.

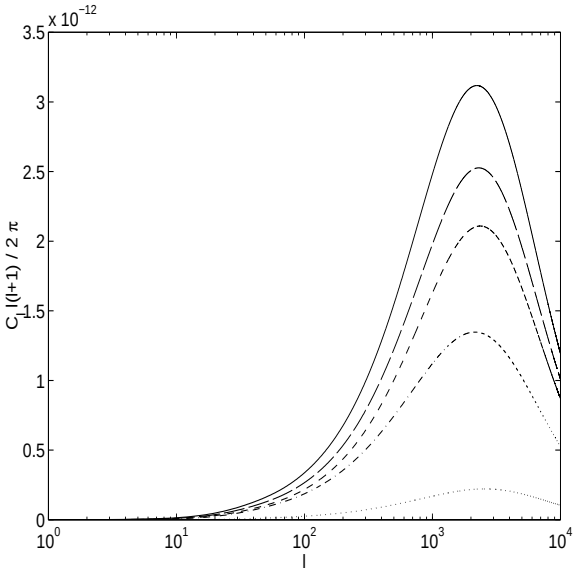

Fig. 4. – Power spectrum predictions for various σ_8 values. Solid, long dashed, short dashed, dashed-dotted and dotted curves correspond to $\sigma_8 = 1.32, 1.23, 1.18, 1.00, 0.68$, respectively.

Along with calculations of the power spectrum, many studies have been conducted of cluster number counts; the detailed predictions for these too show a large variance. Colafrancesco et al. (1997) used a ΛCDM model ($\Omega_0 = 0.2, \Omega_\Lambda = 0.8, h = 0.5, n = 1$) and four different flux limits ($10 - 60\, mJy$) to assess the distribution of cumulative number counts as a function of redshift. Their calculations were carried out within the framework of both evolving and non-evolving IC gas scenarios; for a flux limit of $30\, mJy$ they found cumulative counts of $\sim 2 \cdot 10^4$ clusters to a redshift of $z \sim 0.1$ in the non-evolving gas scenario, and $\sim 4 \cdot 10^3$ clusters when IC evolution is taken into account. In both models counts drop drastically around $z \sim 1$, but with the number of clusters at higher redshifts still much larger in the non-evolutionary case. Number counts exhibit the same degree of sensitivity to σ_8 as the power spectrum; a graphical demonstration of this effect is shown in fig. 5.

In fact, while it is relatively easy to run a code with various input data and examine the resulting output, what is of practical interest is to follow the reverse course, which is obviously much more difficult to implement. Unfortunately, and in contrast with the power spectrum of the primary anisotropy, the shape of the S-Z power spectrum is rather

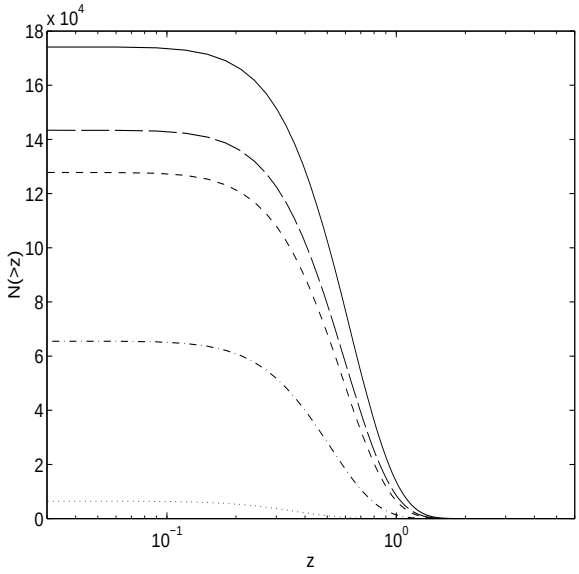

Fig. 5. – Cumulative number counts in redshift space as a function of σ_8. The curves correspond to the same σ_8 values as in fig. 4.

featureless, implying a high degree of model and parameter degeneracy. This means that there are probably several parameter and model combinations that result in the same shape for the power spectrum. Performing a best likelihood test would necessitate a large collection of parameters characterizing both the background cosmology (e.g. Ω_m, Ω_Λ, h), the large scale structure (σ_8), and cluster properties (*e.g.* IC gas morphology, temperature, evolution). The situation will improve significantly when high quality, resolved S-Z and X-ray measurements of individual clusters are available, along with more precisely determined cosmological parameters deduced from independent CMB experiments and large scale structure surveys. Various aspects of the task of removing parameter degeneracies in the analysis of S-Z and X-ray databases have been explored. Mei & Bartlett (2003) have studied the possibility of removing the notorious Ω_m - σ_8 degeneracy by combining the angular correlation function of S-Z clusters with the observed local abundance of X-ray clusters. Diego & Majumdar (2004) have shown how the observed S-Z power spectrum and number counts can be combined to construct a "hybrid power spectrum" whose advantage over the conventional power spectrum is its milder sensitivity to σ_8 and the basic cosmological parameters, thereby increasing its diagnostic power of intrinsic cluster properties. Needless to say, there is still much room for further theoretical study of S-Z power spectrum and number counts in order to devise optimal methods of analysis of the wealth of high quality S-Z measurements expected in the near future.

4. – Measurements

In the first two decades following the discovery of the S-Z effect measurements were made with single dish ground-based telescopes. These observations (which were reviewed in Birkinshaw 1999) are plagued by the need to account for the fluctuating atmospheric emission. Observational and modeling uncertainties are particularly bothersome when

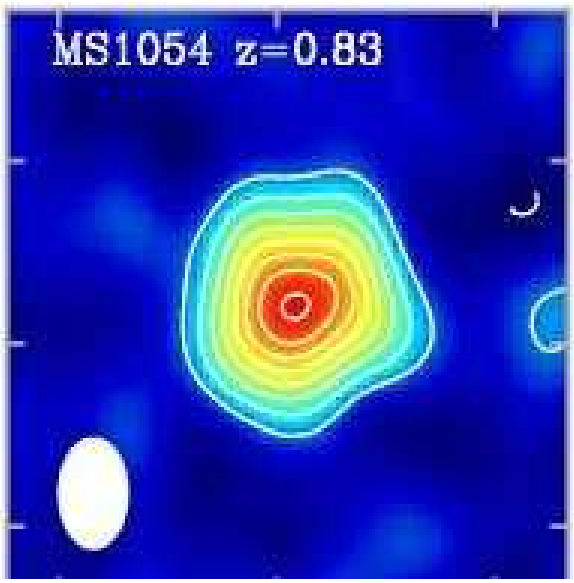

Fig. 6. – S-Z image of the cluster MS1054 obtained by observations at 28.5 GHz with the interferometric BIMA array (from Carlstrom et al. 2002). Colors mark the magnitude of the (negative) intensity change, which is highest (red) in the cluster center.

observations are made at a single frequency. Multi-frequency measurements are essential for separating out the various contributing signals, including atmospheric emission, emission from Galactic dust, cluster radio sources, and CMB anisotropy.

Most observational work during the last decade has been made with interferometric arrays, whose major advantages over single dish telescopes are increased sensitivity to specific angular scales and to signals which are correlated between array elements, insensitivity to changes in atmospheric emission, and high angular resolution on small scales (which is needed to subtract signals from discrete radio sources). The improved sensitivity of radio receivers made it feasible - mainly through the use of low-noise HEMT amplifiers - to image the effect in moderately distant clusters, first with the Ryle telescope (Jones et al. 1993), and then mostly with the BIMA and OVRO arrays (Carlstrom et al. 1996, 2001). Extensive observations (reviewed by Carlstrom et al. 2002) with the latter two arrays, operating at frequencies ~ 30 GHz, yielded high S/N images of some 60 clusters in the redshift range $0.17 < z < 0.89$, one of which is shown in fig. 6.

Interferometric S-Z observations were made also with the CBI, an array of 13 small (0.9 m) dishes, with $3' - 10'$ resolution, operating in the $26 - 36$ GHz spectral range. In contrast to the BIMA and OVRO arrays, the compact configuration of the CBI makes this imager suitable for observations of nearby clusters. Results from measurements of the effect in 7 nearby clusters were reported by Udomprasert et al. (2004).

Multi-frequency measurements of the effect (on the R-J and Wien sides) are, of course, highly desirable for both the extraction of additional information from its spectral shape, and for separating the signal out from the various sources of confusion. The SuZIE experiment is the first multi-element array operating at high frequencies. Some fifteen clusters were observed at three frequency bands (centered on 150, 220, and 350 GHz) with the (two versions of the) experiment (Holzapfel et al. 1997a, 1997b, Mauskopf et

al. 2000, Benson et al. 2004). High frequency measurements were also made with the balloon-borne PRONAOS (Lamarre et al. 1998) - the first detection of the S-Z effect from the stratosphere - and ground-based MITO (De Petris et al. 2002) experiments. Finally, high spatial resolution measurements of the effect in the very luminous cluster RX J13471145 were made with the NOBA and SCUBA bolometer arrays (Kitayama et al. 2004).

5. – Results from S-Z & X-ray Measurements

The main virtues of the S-Z effect that make it a uniquely important cosmological probe are its physically well understood origin and its (essentially) redshift independence. High sensitivity measurements of individual clusters directly yield the integrated pressure of hot IC gas, and thereby also the total mass of the cluster. In general, IC gas density and temperature profiles outside the cluster central region can be more directly obtained from spatially resolved S-Z measurements of $\Delta I_t(r)$ than from measurements of the (more steeply falling) X-ray surface brightness profile. When S-Z measurements are made close to the crossover frequency, the cluster velocity along the los can also be deduced.

The angular diameter distance, and therefore H_0, can be determined from S-Z and X-ray measurements. This SZX method to measure H_0 has clear advantages over the traditional galactic distance ladder method; these include its well understood physical nature, and the capability to test that the global expansion is indeed isotropic. It is also possible to determine the principal contributions to Ω - Ω_m, and the currently favored, Ω_Λ - from the Hubble diagram and from the mean value of the gas mass fraction measured in a (sufficiently large) sample of clusters.

The feasibility of detecting clusters at large redshifts strongly motivates carrying out number counts through cluster surveys in order to characterize the population and its cosmological evolution. The power spectrum of the CMB anisotropy induced by clusters can yield important information on the cluster mass function, cluster properties, and the evolution of clusters. Finally, the anisotropy and redshift evolution of the CMB temperature, $T(z)$, can be determined from multi-frequency measurements of the effect in clusters at different sky directions and redshifts.

In the following subsections we review some of the recent results obtained from current S-Z measurements. The discussion here is *very brief* and devoid of any considerations of important observational issues, such as impact of confusing signals and related systematic uncertainties. Observational aspects are expertly reviewed and assessed by Birkinshaw in this volume. Comprehensive discussions of results from observational S-Z work can be found in the reviews by Birkinshaw (1999) and Carlstrom et al. (2002).

The gas mass fraction f_g: The los integrated gas density can be directly determined if the projected temperature profile is known from spatially resolved spectral X-ray measurements. For a relaxed cluster the measured gas density and temperature can be used in the hydrostatic equation to deduce the total cluster mass $M(r)$ interior to a radial position r. The ratio of the gas to total cluster mass, f_g, is a good measure of the baryonic mass fraction of the cluster, f_b. Determining this ratio for a sufficiently large region, such as r_{500} - the radius at which the mean mass density of the cluster is 500 times the background value - (not only well samples this fraction in the cluster but also) provides a fair estimate of the universal value of the baryonic density parameter (*e.g.* Evrard 1997) when averaged over a sufficiently large sample of clusters. Current best S-Z estimate for f_g is based on BIMA and OVRO measurements of 18 intermediate distance ($0.14 < z < 0.83$)

clusters, which yield $f_g h \simeq (0.08 \pm 0.01) h^{-1}$ for the currently favored matter, $\Omega_m = 0.3$, and cosmological constant, $\Omega_\Lambda = 0.7$, density parameters (Grego et al. 2001). The dependence of the gas fraction on the cluster angular diameter distance can be used to determine Ω_m. Analysis of the above dataset yielded the estimate $\Omega_m \sim 0.25$ in a flat Λ dominated model with $h = 0.7$.

H_0 and Ω: The Hubble constant can be determined from measurement of the angular diameter distance of a cluster, d_A, from resolved S-Z and X-ray observations. When the observed clusters span a wide redshift range, the main contributions to the density parameter - Ω_m and Ω_Λ - can then be deduced from the Hubble diagram (a plot of $d_A(z)$). Analysis of a database of 38 measured distances to 26 clusters (from single dish and interferometric BIMA & OVRO measurements) at redshifts $z \leq 0.83$ yielded a mean value of $H_0 = 60 \pm 3\ kms^{-1}\ \mathrm{Mpc}^{-1}$ for a flat model with $\Omega_M = 0.3$ and $\Omega_\Lambda = 0.7$ (Carlstrom et al. 2002). This $\sim 5\%$ (1σ) observational error is much smaller than the estimated systematic uncertainty of $\sim 30\%$. Contributions to the latter include the unknown gas thermal profile, the assumptions of sphericity of the gas spatial configuration, possible small scale clumping, confusion due to CMB primary anisotropy, and the (unknown) cluster peculiar motion (see Birkinshaw 1999 for details).

Clearly, in order for this method for the measurement of H_0 to yield a value whose level of precision is comparable to those obtained by the local distance ladder, the CMB anisotropy, and SN Ia methods, the overall level of uncertainty has to be lowered to $\sim 5\%$. This could be attained when high quality resolved measurements of a large sample of clusters are made. In order to achieve optimal level of overall systematic uncertainty, the sample must include many *nearby* clusters.

Cluster velocities: Measurements of cluster radial velocities (in the CMB frame) from the kinematic S-Z component necessitate sensitive observations in a narrow spectral band near the crossover frequency (where the thermal component vanishes). The exact spectral shape of the thermal component near this frequency needs to be known. Confusing signals due to the CMB primary anisotropy may very well be the main limitation in reaching levels of precision of a few hundred km/s. Attempts to measure radial velocities using this method were made mostly with the SuZIE experiment (Holzapfel et al. 1997b, Mauskopf et al. 2000, Benson et al. 2003). The SuZIE radial velocity sample includes 8 clusters with velocities in a wide range, with uncertainties so large that none of the deduced values are statistically significant.

CMB temperature: Measurements with the COBE/FIRAS experiment have shown that the CMB spectrum is a precise Planckian with $T_0 = 2.725 \pm 0.002$ K at the current epoch (Mather et al. 1999). In the standard cosmological model, $T(z) = T_0(1 + z)$, a fundamental relation which has not yet been fully confirmed observationally. Cosmological models with a purely blackbody spectrum but with a different $T(z)$ dependence than in the standard model are - formally, at least - unconstrained by the FIRAS measurements. Also unconstrained are models with spectral distortions that are now negligible, but may have been appreciable in the past. Thus far $T(z)$ has been determined mainly from measurements of microwave transitions in interstellar clouds in which atoms and molecules are excited by the CMB (*e.g.* LoSecco et al. 2001). The temperature was determined in the Galaxy, as well as in clouds at redshifts up to $z \sim 3$. Results are, however, substantially uncertain due to the poorly known physical conditions in the absorbing clouds.

The use of the thermal S-Z effect to measure $T(z)$ was suggested long ago (Fabbri,

Melchiorri & Natale 1978, Rephaeli 1980). The method proposed by Rephaeli is based on the steep frequency dependence of ΔI_t on the Wien side, and the weak dependence of *ratios* of the intensity change at different frequencies on the properties of the cluster. Formally, in the nonrelativistic limit such a ratio is completely independent of the Comptonization parameter. Most of the dependence on the cluster parameters drops out also in the exact relativistic description, but a weak dependence remains on the gas temperature; the (unknown) cluster velocity introduces a small systematic uncertainty. S-Z measurements have the potential of yielding more precise values of $T(z)$ than can be obtained from ratios of atomic and molecular lines.

The availability of spectral measurements of the S-Z effect enabled implementation of the method of Rephaeli (1980) to measure $T(z)$ in the Coma and A2163 clusters; the measurements and their analysis are described by Battistelli et al. (2002), and by Melchiorri & Olivo-Melchiorri in this volume. Spectral measurements of Coma ($z = 0.0231 \pm 0.0017$) and A2163 ($z = 0.203 \pm 0.002$) at four frequency bands yield three independent intensity ratios for each cluster; all combinations of these ratios were compared to the theoretically predicted values. Fits of the measured ratios to the predicted values were performed, yielding best fit values for the CMB temperature at the redshifts of the two clusters, $T_{Coma} = 2.789^{+0.080}_{-0.065}$ K and $T_{A2163} = 3.377^{+0.101}_{-0.102}$ K (at 68% confidence). These values are consistent with those expected from the standard relation $T(z) = T_0(1 + z)$. Battistelli et al. (2002) have also tested two alternative scaling relations that are conjectured in non-standard cosmologies, $T(z) = T_0(1 + z)^{1-a}$, and $T(z) = T_0[1 + (1 + d)z]$ (e.g., Lima et al. 2000). They determined the best fit values for the two parameters to be $a = -0.16^{+0.34}_{-0.32}$, and $d = 0.17 \pm 0.36$ (at 95% confidence), values that are consistent with zero, so no significant deviation was found from the standard model. LoSecco et al. (2001) obtained $a = -0.05 \pm 0.13$ and $d = 0.10 \pm 0.28$ (at 95% CL) from measurements of microwave transitions. The two sets of results are consistent. Thus, the S-Z results of Battistelli et al. (2002) already provide the same level of precision even though the two clusters are at much lower redshifts than the galaxies in the sample used by LoSecco et al. (2001). With more precise spectral S-Z measurements expected in the future, it is anticipated that the S-Z method will provide a preferred alternative to the atomic and molecular lines method.

6. – Prospects for the Near Future

The quality of the scientific yield from the many S-Z images obtained with the interferometric BIMA and OVRO arrays proved beyond doubt that the S-Z effect is an indispensable cosmological probe whose great potential has just begun to be exploited. New projects have either already begun observations of the S-Z effect or will become operational in the next few years. These include the ground based AMI, ACT, AMiBA, APEX, MAD/MITO, and SPT, the stratospheric project OLIMPO, and the Planck satellite, whose full sky survey is expected to result in the detection of thousands of clusters (as reviewed by Hansen in this volume).

With the much improved multi-frequency and high spatial resolution capabilities of essentially all the new S-Z projects, the effect will be mapped in many hundreds of clusters, in both pointed and survey modes, thereby greatly enhancing the scope of the measurements and the quality of the scientific yield. Deep, high resolution measurements of the effect in many nearby clusters will provide the best database for precise characterization of the S-Z properties of clusters. The detailed spectral and spatial images will not only yield state-of-the-art gas and total mass profiles, but will also provide us with

the key knowledge to assess and reduce the overall level of systematic uncertainties. This will lead to a great improvement in the precision of the derived values of cluster masses and of the Hubble constant. Extensive cluster surveys and the measurement of the S-Z induced CMB anisotropy will yield the mass and redshift distributions of clusters. Important information will be extracted on the evolution of clusters and the large scale structure. Cosmological parameters, including the dark energy content of the universe, will be determined at a high level of precision.

REFERENCES

[1] Battistelli, B.S., et al. 2002, ApJ, 580, L101
[2] Birkinshaw M. 1999, Phys. Rep., 310, 97
[3] Bartlett J., & Silk J., 1994, ApJ, 423, 12
[4] Benson, B.A. 2003, ApJ, 592, 674
[5] Benson, B.A. 2004, ApJ, 617, 829
[6] Bond J.R., Ruetalo M.I., Wadsley J.W., & Gladders M.D.,2002, *ASPC*, 257, 15
[7] Carlstrom, J.E., Joy, M., & Grego, L. 1996, ApJ, 456, L75
[8] Carlstrom,J.E., Holder, G.P., & Reese, E.D. 2002, ARA& A, 40, 643
[9] Challinor, A., & Lasenby, A. 1998, ApJ, 499, 1
[10] Challinor, A.D., Ford, M.T., & Lasenby, A.N. 2000, MNRAS, 312, 159
[11] Chandrasekhar, S. 1950, 'Radiative Transfer', Oxford, Clarendon Press
[12] Colafrancesco S., Mazzotta P., Rephaeli Y., & Vittorio N. 1994, ApJ, 433, 454
[13] Colafrancesco S., Mazzotta P., Rephaeli Y., & Vittorio N., 1997 ,ApJ, 479, 1
[14] Cooray A., Hu W., & Tegmark M., 2000, ApJ, 540, 1
[15] Cooray, A., & Baumann, D. 2003, Phys. Rev. D, 67, 063505
[16] da Silva A.C., Barbosa D., Liddle A.R., & Thomas P.A. 2000, MNRAS, 317, 37
[17] De Petris, M., et al. 2002, ApJ, 574, L119
[18] Diego, J. M., Mazzotta, P., & Silk, J. 2003, ApJL, 597, L1
[19] Diego J.M., & Majumdar S., 2004, MNRAS, 352, 993
[20] Evrard, A. 1997, MNRAS, 292, 289
[21] Fabbri, R., Melchiorri, F., & Natale, V. 1978, ApS&S, 59, 223
[22] Grego, L., et al. 2001, ApJ, 552, 2
[23] Holzapfel, W.L., et al. 1997a, ApJ, 480, 449
[24] Holzapfel, W.L., et al. 1997b, ApJ, 481, 35
[25] Hu, W. 2000, ApJ, 529, 12
[26] Hughes, J.P., & Birkinshaw, M., 1998, ApJ, 501, 1
[27] Itoh, N., Nozawa, S., & Kohyama, Y. 2000, ApJ, 533, 588
[28] Itoh, N., & Nozawa, S. 2004, A&A, 417, 827
[29] Jones, M., et al. 1993, Nature, 365, 320
[30] Kamionkowski, M., & Loeb, A. 1997, PRD, 56, 4511
[31] Kitayama, T., et al. 2004, Pub. Astron. Soc. Japan, 56, 17
[32] Komatsu E., & Kitayama T. 1999, ApJ, 526, 1
[33] Komatsu E., & Seljak U. 2002, MNRAS, 336, 1256
[34] Lamarre, J.M., et al. 1998, ApJ, 507, L5
[35] Lavaux, G., Diego, J.M., Mathis, H., & Silk, J. 2004, MNRAS, 347, 729
[36] Lee J., & Shandarin S.F. 1999, ApJ, 517, 5
[37] Lima, J.A.S., et al. 2000, MNRAS, 312, 747
[38] LoSecco, J.M., & 2001, Phys. Rev. D 64, 123002
[39] Makino N., & Suto Y. 1993, ApJ, 405, 1
[40] Mather, J.C., et al. 1995, ApJ, 512, 511
[41] Mauskopf, P., et al. 2000, ApJ, 538, 535
[42] Mei S., & Bartlett J.G. 2003, A&A, 410, 767

[43] Molnar S.M., & Birkinshaw M. 2000, ApJ, 537, 542
[44] Nozawa, S., Itoh, N., & Kohyama, Y. 1998a, ApJ, 502, 7
[45] Nozawa, S., Itoh, N., & Kohyama, Y. 1998b, ApJ, 508, 17
[46] Ohno, H., Takada, M., Dolag, K., Bartelmann, M., & Sugiyama, N. 2003, ApJ, 584, 599
[47] Press W.H., & Schechter P. 1974, ApJ, 187, 425
[48] Rephaeli Y. 1980, ApJ, 241, 858
[49] Rephaeli Y. 1981, ApJ, 245, 351
[50] Rephaeli Y. 1995a, ARA& A, 33, 541
[51] Rephaeli Y. 1995b, ApJ, 445, 33
[52] Rephaeli, Y., & Yankovitch, D. 1997, ApJL, 481, L55
[53] Sadeh,S., & Rephaeli, Y. 2004, New Astronomy, 9, 159
[54] Sazonov, S.Y., & Sunyaev, R. A. 1998, ApJ, 508, 1
[55] Sazonov, S.Y., & Sunyaev, R. A. 1999, MNRAS, 310, 765
[56] Sheth R.K., & Tormen G. 1999, MNRAS, 308, 119
[57] Shimon, M., & Rephaeli, Y. 2004, New Astronomy, 9, 69
[58] Shimon M., Rephaeli Y., O'Shea B.W., & Norman M. L. 2005, submitted
[59] Springel V., White M., & Hernquist L. 2001, ApJ, 549, 681
[60] Sunyaev R. 1977, Comm. Ap. Sp. Phys., 7, 1
[61] Sunyaev, R.A., & Zeldovich, Y.B. 1972, Comm. Ap. Sp. Phys., 4, 173
[62] Sunyaev, R.A., & Zeldovich, Y.B. 1980, MNRAS, 190, 413
[63] Udomprasert, P.S., et al. 2004, ApJ615, 63
[64] Weymann R. 1966, ApJ145, 560
[65] Wright E.L. 1979, ApJ, 232, 348-351
[66] Zeldovich, Y.B., & Sunyaev, R.A. 1969, Astrophys. Sp. Sci., 4, 30l
[67] Zhang P., Pen, U.L., & Wang B. 2002, ApJ, 577, 555